Nanoscale

Cite this: *Nanoscale*, 2012, **4**, 4107

www.rsc.org/nanoscale

**COMMUNICATION**

# A DNA-templated fluorescent silver nanocluster with enhanced stability†

**Jaswinder Sharma,[a] Reginaldo C. Rocha,[a] M. Lisa Phipps,[a] Hsin-Chih Yeh,[a] Kirill A. Balatsky,[a] Dung M. Vu,[b] Andrew P. Shreve,[c] James H. Werner[a] and Jennifer S. Martinez*[a]**

***Received 19th March 2012, Accepted 5th May 2012***
**DOI: 10.1039/c2nr30662j**



**We report the discovery of a DNA sequence that templates a highly stable fluorescent silver nanocluster. In contrast to other DNA templated silver nanoclusters that have a relatively short shelf-life, the fluorescent species templated in this new DNA sequence retains significant fluorescence for at least a year. Moreover, this new silver nanocluster possesses low cellular toxicity and enhanced thermal, oxidative, and chemical stability.**

Fluorescent reporters, such as organic dyes, quantum dots, and fluorescent proteins, are incredibly useful tools for cellular biology that enable direct visualization of cellular and biomolecular processes that would otherwise be invisible to the naked eye.[1–3] Techniques such as confocal microscopy, single particle tracking, and single molecule spectroscopy have shed significant light on biomolecular processes such as protein folding and cellular signaling.[4] While substantial progress has been made utilizing conventional organic dyes, fluorescent proteins, and quantum dots as biomolecular labels, each of these fluorescent probes has limitations.[1–3] The ideal fluorescent probe would be substantially smaller than the biomolecule to which it is attached, as photostable as a quantum dot, and could be templated in biomolecules *in situ*. One promising and relatively new class of fluorescent probe, that has the potential to simultaneously meet many of these stringent criteria, are fluorescent nanoclusters of silver or gold.[5–8]

Gold and silver nanoclusters are collections of a small number of metal atoms (typically <2 nm).[5–8] Gold nanoclusters have a rich history of study with intriguing structural ligation, as well as fluorescence, near IR activity and catalytic properties.[9–13] However, the use of silver nanoclusters as biolabels is gaining increasing attention, as these fluorescent species can be synthesized in biologically relevant ligands and directly synthesized using DNA as a template.[14–16] DNA-templated fluorescent Ag nanoclusters (AgNCs) typically consist of less than ~20 silver atoms as determined by mass spectrometry, elemental analysis, and Ag K-edge EXAFS.[17–19] These AgNCs can be produced as a palette of different wavelengths[20,21] and their use as fluorophores in protein,[22] DNA,[23,24] and metal ion[25–27] detection is only in its infancy. However, most AgNCs suffer from short shelf-lives as a result of facile oxidation by air/$O_2$, which can limit their use as biological labels.[17,21,28] Further, the most stable clusters tend to be green emitting AgNCs (which usually indicates an oxidized cluster). These green oxidized AgNCs typically have lower quantum yields than red-emitting AgNCs and also emit in a spectral region that has substantial overlap with cellular and tissue autofluorescence.[18,21,28] Due to these shortcomings, the creation of a AgNC that has a long shelf-life and is highly stable when challenged with temperature, oxidation, and pH is highly desirable. In this work, we report the DNA sequence, 5′-ACCCGAACCTGGGCTACCACCCT TAATCCCC-3′ termed D′ (the prime designates apo DNA), that can template a silver nanocluster that retains significant fluorescence for at least a year and is highly resistant to oxidation, pH, and temperature. In addition, cell viability is substantially higher in the presence of this cluster than in the presence of less stable DNA-templated silver nanoclusters.

AgNCs formed from D′ (D-AgNC) are highly fluorescent moieties with a fluorescence quantum yield of 30% (Experimental details, Section S1, ESI†). The emission peak of D-AgNC does not substantially change as a function of excitation wavelength (Fig. S1†), suggesting formation of a single emissive species.[17] Further, D-AgNC exhibits much greater fluorescence stability as compared to previously reported AgNCs (Fig. 1). After 168 h in dark storage at room temperature, D-AgNC retains 75% of the initial fluorescence intensity, whereas previously reported clusters retained ~3 to 20%. D-AgNC maintained ~75% of the initial fluorescence for an additional 100 days and still remained 31% fluorescent after ~10 months of dark storage at room temperature (Fig. 2a). The apparent fluorescence increase for J15-AgNC results from oxidation and blue-shifting of the emission wavelength (all AgNC were formed and sealed under ambient air). Most of the previously reported AgNCs (J1–J13′) blue-shifted over time (Fig. 1a). In contrast to previously reported AgNCs, the emission wavelength of D-AgNC has not shown blue shifts with time (~10 months). D-AgNC was also very stable at higher temperatures (Fig. 2b). Employing a real-time thermocycler, we observed that D-AgNC maintains 50% of the initial fluorescence up to 80 °C while other AgNCs are stable only below 60 °C (Fig. 2b).

[a]*MPA-Center for Integrated Nanotechnologies, Los Alamos National Laboratory, MS K771, Los Alamos, NM 87545, USA. E-mail: jenm@lanl.gov; Fax: +1-505-665-9030; Tel: +1-505-665-0045*
[b]*C-PCS, Los Alamos National Laboratory, Los Alamos, NM 87545, USA*
[c]*Center for Biomedical Engineering and Department of Chemical and Nuclear Engineering, University of New Mexico, Albuquerque, NM 87131, USA*

† Electronic supplementary information (ESI) available: Experimental conditions, DNA sequences, effect of light and oxygen, additional electrochemical data, and data from *in vivo* studies on AgNCs. See DOI: 10.1039/c2nr30662j

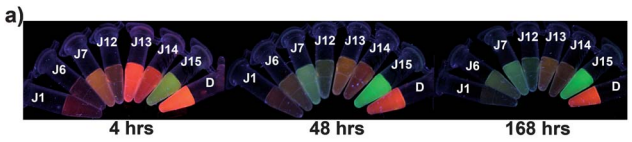


b) Table 1. Fluorescence of different AgNCs at different time intervals.

| AgNC | $\lambda_{Exc}/\lambda_{Emi}$ (nm) | Fluor. 4 hrs (a.u.) | Fluor. 48 hrs (a.u.) | Fluor. 168 hrs (a.u.) | % Fluor. 48 hrs | % Fluor. 168 hrs |
|---|---|---|---|---|---|---|
| J1 | 575/635 | 3826.96 | 1749.68 | 448.25 | 45.71 | 11.71 |
| J6 | 560/620 | 1672.28 | 891.39 | 347.10 | 53.30 | 20.75 |
| J7 | 550/630 | 3057.71 | 511.46 | 128.36 | 16.72 | 4.19 |
| J12 | 545/605 | 3645.86 | 430.23 | 88.59 | 11.80 | 2.42 |
| J13 | 595/655 | 18616.72 | 3751.00 | 683.89 | 20.14 | 3.67 |
| J14 | 640/700 | 23164.22 | 7594.35 | 1408.47 | 32.78 | 6.08 |
| J15 | 405/525 | 2240.63 | 2883.44 | 3149.67 | 128.68 | 140.57 |
| D | 535/615 | 13565.62 | 10711.21 | 10220.03 | 78.95 | 75.33 |

**Fig. 1** D-AgNC is more stable than preceding AgNCs. (a) Photographs showing the fluorescence of AgNCs at different time intervals. (b) Table showing integrated fluorescence. The apparent fluorescence increase for J15 results from oxidation and blue shifting.

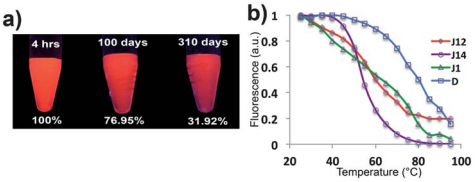


**Fig. 2** Stability of D-AgNC with time and temperature. (a) Photographs and percent fluorescence (relative to initial intensity) as a function of time. (b) Fluorescence as a function of temperature.

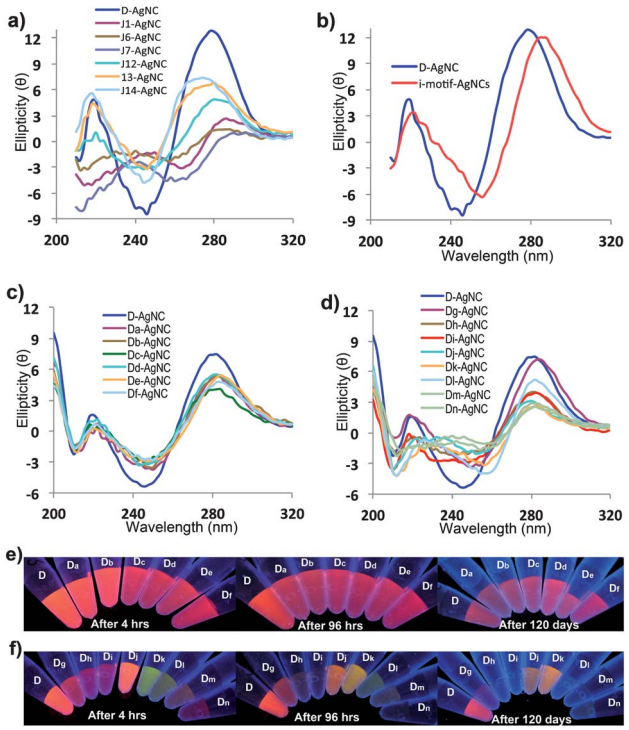


**Fig. 3** CD studies of D-AgNC, its evolved sequences, and some of the previous AgNCs. (a) D-AgNC and some previously reported AgNCs. (b) I-motif stabilized AgNC and D-AgNC: D′ stabilizes AgNC differently from previously characterized DNA sequences and it is not i-motif forming. (c) D-AgNC and Da–Df-AgNC: similar temporal stability equates to similar secondary structure. (d) D-AgNC and Dg–Dn-AgNC. (e) Photographs of the stable D-AgNC and Da–Df-AgNC as a function of time. (f) Photographs of D-AgNC and Dg–Dn-AgNC as a function of time.

We compared secondary structure of the DNA template of different AgNCs *via* circular dichroism (CD) spectroscopy (Experimental details, Section S1†). D-AgNC exhibits different secondary structure as compared to previously published DNA-templated AgNCs (Fig. 3a). The CD spectra of D-AgNC and its related corollaries do not have features at 260 nm (−ve ellipticity) nor 290 nm (+ve ellipticity), which are specific spectral features for DNA i-motifs found for many other DNA-templated silver nanoclusters.[29,30] Similarly, absence of any +ve peak (parallel G-quadruplexes) or −ve peak (antiparallel G-quadruplexes) at 260 nm and +ve peak at 290 nm indicates the absence of G-quadruplex like secondary structure (Fig. 3b).[30] Consistent with lack of i-motif structures, D-AgNC and related AgNCs are stable between pH 6.5–10 (Fig. S2†), whereas i-motif DNA structure (DNA-templated AgNCs) are stable at low pH (<6.0). Thus, D-AgNC has high temporal, temperature, and pH stability.

The D′ DNA templating sequence was systematically altered to better understand the role of specific DNA bases in controlling the emission and stability of D-AgNCs (DNA sequences are provided in the ESI, Section S1†). Removal of the presumed nanocluster templating sequence (D–D′) eliminates cluster formation (Fig. S7†). Further, randomization of the D′ sequence, while maintaining the same number of adenine, guanine, cytosine, and thymine bases, did not template AgNCs with any substantial fluorescence or enhanced stability (Fig. S3†). Substitution in D′ of the 5′-A with C, G, or T did not change fluorescence stability or emission wavelength (Fig. S6†). Similarly, random deletion of bases from sequence D resulted in reduced stability and shifted emission wavelength (Fig. S7†). Internal deletions of up to six individual bases between the nanocluster templating sequence and the 5′ sequence (Da–Df′) had little effect on stability, fluorescence wavelength, or CD spectra (Fig. 3c and e and S5†). However, proximal 5′ internal (Dg–Dn′) or external (D2–D11′) deletions led to significant changes in fluorescence and stability, with concomitant differences in secondary structure of the templating DNA, as determined by CD (Fig. 3d and f, S4 and S5†). Thus, bases in Da–Df do not seem to play any significant role in stabilizing the AgNCs while bases in Dg–Dn play a significant role in maintaining stability and fluorescence intensity. The internal positions, with their tolerance to deletion, have been shown to be ideal locations for attachment of D-AgNC to solid surfaces (through biotinylation) with retention of fluorescence.

Motivated by observations that D-AgNC exhibits enhanced resistance against spontaneous oxidation by air/$O_2$, we have initiated electrochemical studies by cyclic voltammetry. The cyclic voltammograms (CV) in Fig. 4 and S8† show a single anodic process corresponding to the totally irreversible metal-based oxidation of the nanocluster (*i.e.*, $Ag_n \rightarrow Ag_n^+ + e^-$). This oxidation peak appears only in the first forward scan, and no reduction peak is observed in the backward scan. Also confirming the electrochemical irreversibility of the system is the clear exponential dependence of the oxidation peak potential ($E_p$) on the potential scan rate ($v$),[31] with $E_p$ shifting to more positive values as $v$ increases (Fig. 5 and S8†). Since the anodic

 

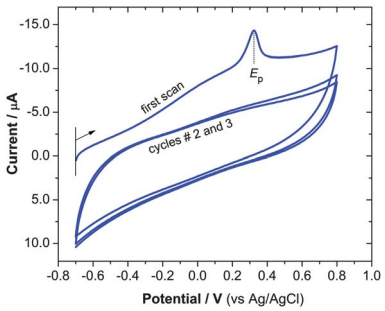


**Fig. 4** Typical cyclic voltammogram of D-AgNC in 50 mM PB pH 6.8 (CV at $v = 500$ mV s$^{-1}$, see Fig. S8† for CVs at various scan rates).

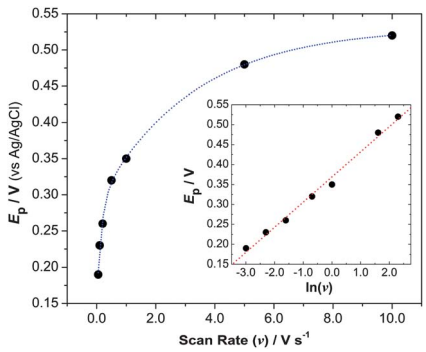


**Fig. 5** The dependence of peak potentials ($E_p$) on the scan rate ($v$) of CVs for the irreversible electrochemical oxidation of D-AgNC.

current peak $E_p$ varies with the scan rate $v$ in the CVs, the oxidation potential ($E_{ox}$) of D-AgNC was determined from the plot of $E_p$ *vs.* $v$ (Fig. 5) by extrapolation of the $E_p$ value at the intercept of $v = 0$ ($E_{ox} = +0.15$ *vs.* Ag/AgCl; +0.35 V *vs.* NHE). Such a positive $E_{ox}$ elucidates the thermodynamic stability of the reduced fluorescent D-AgNC species as well as its high resistance to oxidation by air.

The redox behavior of D-AgNC is overall consistent with a slow heterogeneous electron transfer to the electrode followed by a fast homogeneous chemical process, which is clearly indicated by the absence of a reduction peak in the cathodic reverse scan (Fig. 4 and S8†). Because the $Ag_n^+$ species is rapidly consumed in an electrochemically coupled reaction upon the first anodic cycle, no cathodic activity for a subsequent reduction ($Ag_n^+ + e^- \rightarrow Ag_n^0$) can be seen even if CVs are run at potential scan rates as fast as >10 V s$^{-1}$. Our tests suggest that the fluorescent $Ag_n^0$ species can be regenerated by bulk chemical (re)reduction of an oxidized sample using $NaBH_4$ as reductant, but the kinetics for this (re)formation reaction appears to be too slow for significance on the time scale of our CV measurements.

Preliminary bulk electrolyses have also confirmed that the intense fluorescence of D-AgNC vanishes quickly with oxidation upon application of potentials more positive of $E_{ox}$ (*e.g.* $E_{app} = +0.5$ V). Attempts toward the electrolytic (re)reduction of the oxidized products (by negatively reversing the application of potential) proved to be inefficient in regenerating the fluorescent species. Combined with the results from CV, these experiments provide additional evidence that the (re)formation of fluorescent NCs is limited by slow kinetics, which is generally characteristic of multi-step transformations comprising complex mechanisms. In order to gain a deeper understanding of

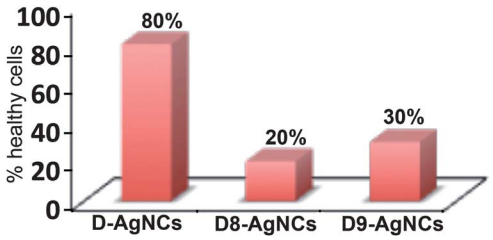


**Fig. 6** Increased stability toward time, temperature, pH, and oxidation correlate with increased biocompatibility. Percent healthy cells after addition of 5 μM AgNC to macrophages. Live/dead analysis (Fig. S9†) correlates to observational health.

such findings as well as to explore the interdependency of redox and optical activities in detail for D-AgNC, further systematic studies *via in situ* spectroelectrochemical approaches are underway.

Given the increased temporal, pH, temperature, and oxidative stability of D-AgNC, we were curious to see if this enhanced stability in any way made these nanoclusters less toxic to live cells as compared to less stable DNA templated AgNCs. Our preliminary experiments show that D-AgNC is less toxic to macrophages (differentiated THP1 cells: Experimental details, Section S4†). After one hour of treatment, over 80% of the cells exposed to 5-micromolar D-AgNC were still alive and healthy, whereas less than 30% of cells exposed to similar concentrations of D8- and D9-AgNC were still healthy (Fig. 6). Cells treated with D′, D8′, and D9′ DNA were 100% viable. Further, this qualitative assessment correlates with live–dead cell counting (Fig. S9†). AgNCs were not toxic in undifferentiated THP-1 cells. Presumably, the less stable endocytosed clusters release free silver into the cell, which results in greater toxicity.

In conclusion, we have discovered a DNA sequence which templates AgNCs with enhanced shelf-life, pH and thermal stability. Additionally, our electrochemical studies confirmed their oxidation resistance and clearly demonstrated that D-AgNC is highly stable in its fluorescent native state, whereas oxidation leads to instability and optical inactivity. This nucleating DNA sequence and a family of related sequences will open new opportunities for fluorescent silver nanocluster applications that require longer incubation times, high temperature, and consistent fluorescence for longer periods of time. Our investigations indicate that the enhanced stability of these nanoclusters is related to the specific secondary structures achieved by the surrounding DNA strands. Studies of DNA deletions and insertions to this sequence have pointed to the most likely nucleation site on the sequence and have suggested potential attachment sites for future bioconjugation or surface immobilization. Further investigations to understand the extraordinary stability of these AgNCs are in progress in our laboratories.

## Acknowledgements

This research was supported by the Department of Energy, Office of Basic Energy Science, Division of Material Science and Engineering (J.S., R.C.R., A.P.S. and J.S.M.) and LANL's Directed Research and Development (H.C.Y., J.H.W., D.M.V.). This work was performed at the Center for Integrated Nanotechnologies (CINT), a U.S. Department of Energy, Office of Basic Energy Sciences user facility (M.L.P).

## Notes and references


1 B. N. G. Giepmans, S. R. Adams, M. H. Ellisman and R. Y. Tsien, *Science*, 2006, **312**, 217–224.
2 C. Joo, H. Balci, Y. Ishitsuka, C. Buranachai and T. Ha, *Annu. Rev. Biochem.*, 2008, **77**, 51–76.
3 R. H. Newman, M. D. Fosbrink and J. Zhang, *Chem. Rev.*, 2011, **111**, 3614–3666.
4 N. P. Wells, G. A. Lessard, P. M. Goodwin, M. E. Phipps, P. J. Cutler, D. S. Lidke, B. S. Wilson and J. H. Werner, *Nano Lett.*, 2010, **10**, 4732–4737.
5 J. Zheng, P. R. Nicowich and R. M. Dickson, *Annu. Rev. Phys. Chem.*, 2007, **58**, 409–431.
6 I. Diez and R. H. A. Ras, *Nanoscale*, 2011, **3**, 1963–1970.
7 L. Shang, S. Dong and G. U. Nienhaus, *Nano Today*, 2011, **6**, 401–418.
8 S. Kumar, M. D. Bolan and T. P. Bigioni, *J. Am. Chem. Soc.*, 2010, **132**, 13141–13143.
9 D. Lee, R. L. Donkers, G. Wang, A. S. Harper and R. W. Murray, *J. Am. Chem. Soc.*, 2004, **126**, 6193–6199.
10 M. Zhu, C. M. Aikens, F. J. Hollander, G. C. Schatz and R. Jin, *J. Am. Chem. Soc.*, 2008, **130**, 5883–5885.
11 O. Varnavski, R. G. Ispasoiu, L. Balogh, D. Tomalia and T. Goodson, *J. Chem. Phys.*, 2001, **114**, 1962–1965.
12 P. D. Jadzinky, G. Calero, C. J. Ackerson, D. A. Bushnell and R. D. Kornburg, *Science*, 2007, **318**, 430–433.
13 S. Link, A. Beeby, S. FitzGerald, M. A. El-Sayed, G. T. Schaaff and R. L. Wetten, *J. Phys. Chem. B*, 2002, **106**, 3410–3415.
14 C. Guo and J. Irudayaraj, *Anal. Chem.*, 2011, **83**, 2883–2889.
15 J. T. Petty, J. Zheng, N. V. Hud and R. M. Dickson, *J. Am. Chem. Soc.*, 2004, **126**, 5207–5212.
16 B. Han and E. Wang, *Anal. Bioanal. Chem.*, 2012, **402**, 129–138.
17 C. M. Ritchie, K. R. Johnsen, J. R. Kiser, Y. Antoku, R. M. Dickson and J. T. Petty, *J. Phys. Chem. C*, 2007, **111**, 175–181.
18 P. R. O'Neill, L. R. Velazquez, D. G. Dunn, E. G. Gwinn and D. K. Fygenson, *J. Phys. Chem. C*, 2009, **113**, 4229–4233.
19 M. L. Neidig, J. Sharma, H.-C. Yeh, J. S. Martinez, S. D. Conradson and A. P. Shreve, *J. Am. Chem. Soc.*, 2011, **133**, 11837–11839.
20 C. I. Richards, S. Choi, J.-C. Hsiang, Y. Antoku, T. Vosch, A. Bongiorno, Y.-L. Tzeng and R. M. Dickson, *J. Am. Chem. Soc.*, 2008, **130**, 5038–5039.
21 J. Sharma, H.-C. Yeh, H. Yoo, J. H. Werner and J. S. Martinez, *Chem. Commun.*, 2010, **46**, 3280–3282.
22 J. Sharma, H.-C. Yeh, H. Yoo, J. H. Werner and J. S. Martinez, *Chem. Commun.*, 2011, **47**, 2294–2296.
23 H.-C. Yeh, J. Sharma, J. Han, J. S. Martinez and J. H. Werner, *Nano Lett.*, 2010, **10**, 3106–3110.
24 G.-Y. Lan, W.-Y. Chen and H.-T. Chang, *Biosens. Bioelectron.*, 2011, **26**, 2585–2589.
25 X. Yuan, T. Yeow, Q. Zhang, J. Y. Lee and J. Xie, *Nanoscale*, 2012, **4**, 1968–1971.
26 S. Liu, F. Lu and J.-J. Zhu, *Chem. Commun.*, 2011, **47**, 2661–2663.
27 L. Shang and S. Dong, *J. Mater. Chem.*, 2008, **18**, 4636–4640.
28 S. Choi, J. Yu, S. A. Patel, Y.-L. Tzeng and R. M. Dickson, *Photochem. Photobiol. Sci.*, 2011, **10**, 109–115.
29 B. Sengupta, K. Springer, J. G. Buckman, S. P. Story, O. H. Abe, Z. W. Hasan, Z. D. Prudowsky, S. E. Rudisill, N. N. Degtyareva and J. T. Petty, *J. Phys. Chem. C*, 2009, **113**, 19518–19524.
30 J. Kypr, I. Kejnovska, D. Renciuk and M. Vorlickova, *Nucleic Acids Res.*, 2009, **37**, 1713–1725.
31 A. J. Bard and L. R. Faulkner, *Electrochemical Methods – Fundamentals and Applications*, Wiley, New York, 2nd edn, 2001.


 